JOURNAL OF MATERIALS SCIENCE 18 (1983) 2305–2310

Influence of precracking load on critical stress intensity factor of mild steel

HSING-SHIH CHEN, JI-LIANG DOONG
Department of Mechanical Engineering, National Cheng Kung University, Tainan, Taiwan, ROC

The effects of precracking load on critical stress intensity factor are studied. A plane stress model of elastic/plastic stress distribution which has strain hardening effects included is used. The effects of residual stresses and strain hardening due to fatigue load are calculated by choosing plastic zone size as fracture criterion. And experimental results are obtained to prove the reliability of theoretical calculations. The results show that the influence of fatigue load can be estimated directly by a computer program.

1. Introduction

In the test procedures for critical stress intensity factor measurements, it is recommended to pre-crack the specimen by fatigue. However, the possible effects of residual stress by fatigue are not considered.

In order to establish the role played by residual stress distributions in crack propagation rates, several authors [1, 2] have attempted to calculate and measure the residual stresses by different models and experimental techniques. For example, Elber [3], Adams [4] focused on crack closure phenomena to obtain information on residual stress. A direct measurement of residual stress performed in photoelastic materials is given in the report of Post [5]. Tirosh [6] used a theoretical model, based on dislocation mechanics, to predict the residual stress distribution resulting from fatigue cracking. Using the linear elastic fracture mechanics, Rice [7] suggested a relation for plastic zone size R given by Equation 1.

$$R = 2r_{\mathrm{y}} = \frac{1}{\pi}\left(\frac{K}{\sigma_{\mathrm{y}}}\right)^2 \tag{1}$$

where K is the stress intensity factor and σ_{y} is the yield strength of the material and r_{y} is shown in Fig. 1.

Cyclic loading produces forward and reverse plastic deformation at the crack tip during loading and unloading parts of the cycle, respectively [8] which gives rise to residual strains in the neighbourhood of the crack tip. Elber [9] suggested an effective stress intensity factor at the crack tip, on account of the residual deformations. He used a factor U which is known as the effective stress range factor to evaluate the effect of residual stresses by cyclic loading. Lal [10] presents a model to calculate the plastic zone size at the crack tip using mechanical properties of the material and loading conditions (Mode I). The parameter U controlling the effects of residual deformations has been incorporated. Dahl [11] has studied experimentally the influence of plastic zone size on fracture toughness.

These are few papers which discuss the influence of precrack histories on fracture toughness. This is also true for theoretical analysis. In the present paper, a plane stress model of elastic/plastic stress distribution is used. Strain hardening effects will be considered. The residual stress and plastic zone size after loading and unloading can be calculated by the present model. Critical plastic zone is chosen as the fracture criterion to evaluate the instability of the crack extension. The effects of strain hardening and compressive residual stress within this criterion on fracture toughness can be seen by using the present calculation. Experimental results are obtained to show the reliability of the theoretical calculation. The future studies will show the effects of crack propagation on the residual stress distribution, plastic zone size and fracture toughness.

0022–2461/83 $03.00 + .12

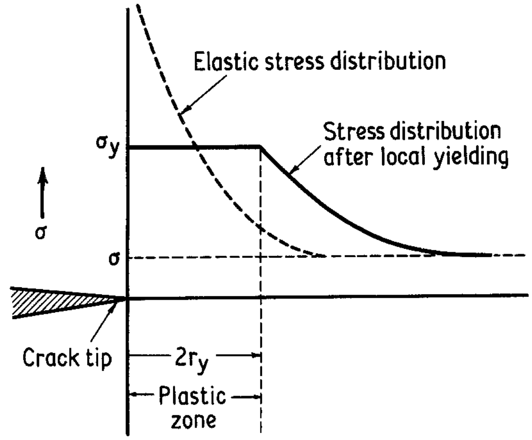

Figure 1 Distribution of the stress component in the crack-tip region.

2. Stress distribution near a crack

The stress distribution in a cracked element can be calculated by the theory of elasticity, with the assumption of linear elastic behaviour. The most simple model is an infinite sheet loaded by a tensile stress σ (as shown in Fig. 2). The Westergaard approach [12] to calculate the stress distribution near a sharp crack is the best method to examine the properties of a particular type of crack. A suitable complex function is chosen to satisfy the boundary conditions and the properties of compatability. The solution of plane stress is an infinite plate with a small crack under uniaxial tension at $y = 0$ is given as follows:

$$S(x) = \sigma/(1-(c/x)^2)^{1/2} \tag{2}$$

The stress distribution of a plane with a finite width $2b$ can be obtained by modifying the solution of a factor $f(c)$ which is derived by making the summation stresses equal to the applied load. This characteristic is shown in Equations 3 and 4

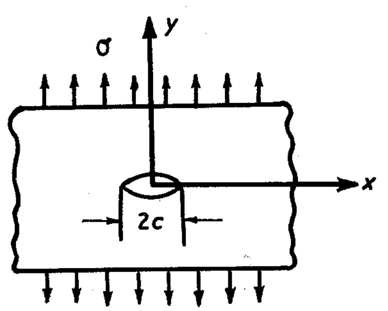

Figure 2 Westergaard's model of a crack under uniaxial tension in an infinite plate.

$$\sigma \cdot 2b = 2\int_c^b \sigma^* x/(x^2-c^2)^{1/2}\,dx \tag{3}$$

$$\sigma^* = \sigma \cdot b/(b^2-c^2)^{1/2} = \sigma \cdot f(c) \tag{4}$$

where $f(c) = b/(b^2-c^2)^{1/2} = 1/[1-(c/b)^2]^{1/2} = 1/(1-N^2)^{1/2}$ in which the dimensionless parameter $N = c/b$ is used.

Analytical solutions of stress distribution in the field of a mixed elastic/plastic field has been obtained for a plane stress model. Considering the elastic stress distribution in plane stress, as shown in Fig. 3 the plastic zone is supposed to extend a distance $D_2 - c$ ahead of the crack tip ($x = c$). Owing to strain hardening, the tensile stress $S(x)$ is assumed to be linearly distributed beyond the yield strength within this zone. So $S(D_2) = \sigma_y$ and we define $S(c) = \sigma_c$. The material outside the plastic zone is assumed to be the same as the elastic stress. The elastic stress is distributed for an imaginary, extended crack of length $2c_1$, which is expressed by curve BC.

Lal [10] has studied the influences of ultimate strength σ_u on plastic tensile instability. It was proved that the area of yielded zone decreases with increasing hardness of the material. He pointed out that as the stress at the crack tip exceeds the ultimate tensile strength of the material, the crack extends further through the plastically deformed region. For this reason, σ_c may be assumed equal to σ_u after fatigue cracking.

The stress distributions over the whole plate under loading condition are shown in Equations 5 and 6,

$$S(x) = (\sigma_c - \sigma_y)(D_2 - x)/(D_2 - c) + \sigma_y \qquad D_2 \geqslant x > c \tag{5}$$

$$S(x) = \sigma \cdot f(c_1)x/(x^2-c_1^2)^{1/2} \qquad x \geqslant D_2 \tag{6}$$

and

$$S(D_2) = \sigma_y,$$

$$\sigma_y = \sigma \cdot f(c_1)D_2/(D_2^2-c_1^2)^{1/2}. \tag{7}$$

The value of c_1 can be determined under the condition that the total loads or curve ABC and curve A′B′C′ are the same,

$$\int_c^b S(x)\,dx = \int_c^b \sigma \cdot f(c)x/(x^2-c^2)^{1/2}\,dx \tag{8}$$

$$\int_c^{D_2} S(x)\,dx + \int_{D_2}^b S(x)\,dx = \sigma \cdot f(c) \times \int_c^b x/(x^2-c^2)^{1/2}\,dx \tag{9}$$

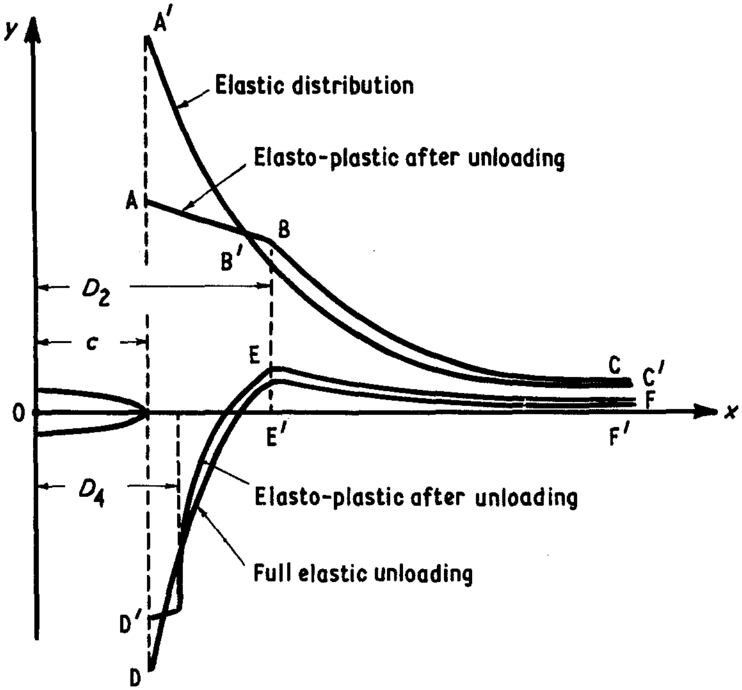

Figure 3 Schematic elastic/plastic stress distribution near a notch after loading and unloading.

$$\tfrac{1}{2}(D_2-c)(\sigma_y+\sigma_c)+\sigma\cdot f(c_1)(x^2-c_1^2)^{1/2}\Big|_{D_2}^{b} = \sigma\cdot f(c)(x^2-c^2)^{1/2}\Big|_{c}^{b} \quad (10)$$

$$\tfrac{1}{2}(D_2-c)(\sigma_y+\sigma_c)-\sigma\cdot f(c_1)(D_2^2-c_1^2)^{1/2} = 0 \quad (11)$$

The two unknowns c_1 and D_2 can be obtained by solving Equations 7 and 11 simultaneously.

If the strip is unloaded, the stress in the plastic zone does not fit with the elastic stress distribution. This misfit causes residual stresses. Full elastic unloading will cause residual compressive stresses at A, exceeding the compressive yield strength. As a result of the unloading process, a reversed plastic deformation will occur between c and D_4. Obviously D_4-c is much smaller than D_2-c. The elastic/plastic stress distribution $R(x)$ and plastic zone size after unloading are solved by the same procedure as the loading condition. Compressive yield strength is assumed to be equal to tensile yield strength. Equations 12 and 13 are used to solve c_2 and D_4.

$$-\sigma_y = \frac{D_2-D_4}{D_2-c}(\sigma_c-\sigma_y)+\sigma_y - \sigma f(c_2)D_4/(D_4^2-c_2^2)^{1/2} \quad (12)$$

$$(\sigma_c+\sigma_y)(D_4-c)+\tfrac{1}{2}(D_4-c)\frac{D_2-D_4}{D_2-c}(\sigma_c-\sigma_y) - \sigma f(c)(D_4^2-c^2)^{1/2} = \sigma f(c_2)(D_4^2-c_2^2)^{1/2} \quad (13)$$

It can be seen that c_2 and D_4 are found by simultaneously solving Equations 12 and 13. If strain hardening effect doesn't exist, then the material within the plastic zone is rigid-perfectly plastic and σ_c is equal to yield strength σ_y. The solutions of D_2' which are based on rigid-perfectly plastic assumption are compared with Rice's solutions in Equation 1. In Fig. 4, plots are made of $(D_2'-c)/R$ against $M=\sigma/\sigma_y$ for various values

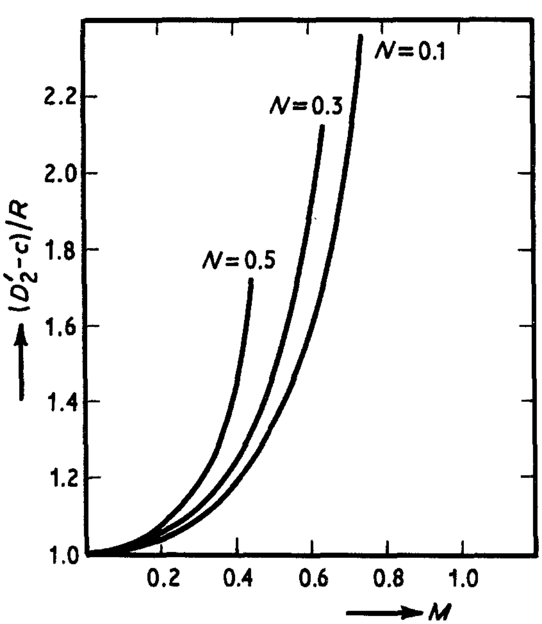

Figure 4 Comparison of $(D_2'-c)/R$ against M for various values of N.

TABLE I Chemical composition of the steel investigated in wt %

C	Si	Mn	P	S	Cr	Ni	V	Cu
0.0758	0.0934	0.2859	0.0037	0.034	0.0417	0.0311	0.0036	0.111

of relative crack length N. It can be seen that the present results agree with Rice's results very well when M and N are small. The difference increases with the crack length or increasing gross stress.

3. Experimental procedure and results

Chemical compositions of the plain carbon steel specimen are given in Table I. Specimens were annealed at 1173 K for 1 h. Fig. 5 shows the size of the specimens which were machined by electric discharge machining. The specimens were precracked to a definite length 18.5 mm under three different load conditions. The method of measuring the K_c values was suggested by reference [13] on a closed loop electrohydraulic testing machine at room temperature. The K_c can be calculated by the following equation [14].

$$K_c = \frac{P \cdot c^{1/2}}{t(2b)} \left(1.77 - 0.1\left(\frac{c}{b}\right) + \left(\frac{c}{b}\right)^2\right) \quad (14)$$

where P is the fracture load and t is the specimen thickness. The results of static tensile tests and K_c values are shown in Fig. 6 and Table II, respectively. The K_c value and the plastic zone size increases with the increasing of $M = \sigma/\sigma_y$. This conclusion coincides with Dahl's results [11].

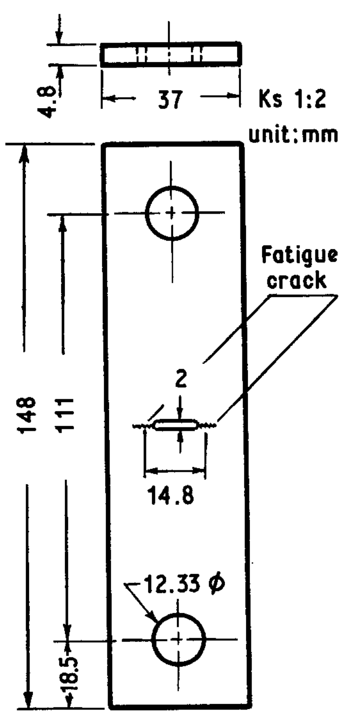

Figure 5 Centre cracked plate's dimensions.

4. The influence of fatigue load on fracture behaviour

There are two reasons to explain the influence of fatigue load on critical stress intensity values. Before our discussion, we should choose a suitable fracture criteria, critical plastic zone ρ_{cr}, to prevent instability crack extension from occurring. Fracture philosophy by means of plastic zone size is similar to the crack opening displacement (COD) concept, but has the advantage that the plastic zone is easily determined by K-value cancellation of the Dugdale crack model [15], and it is convenient to calculate the effects of strain hardening and compressive residual stress on K_c from this criterion directly. It is well known that under plastic deformation when strained to a particular value of the stress, say σ^*_{yp} (see Fig. 6) a number of dislocation sources are activated, as a result of which the dislocation density increases. The resistance to further deformation increases. When the material is released and reloaded, yielding of the material does not take place until the value of the applied stress reaches the value of σ^*_{yp}. In

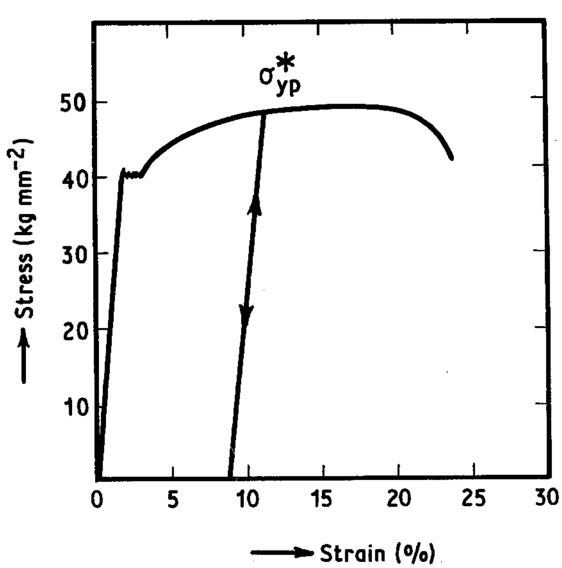

Figure 6 Stress–strain curve.

TABLE II Theoretical and experimental results

M	A (kg)	B (Kg)	P_{ex} (kg)	K_c (kg mm$^{-3/2}$)	P_a (kg)	K_{ca} (kg mm$^{-3/2}$)
0.244	53.94	18.80	3283.09	116.00	3210.34	113.43
0.365	137.31	69.48	3392.55	119.87	3185.76	112.56
0.487	299.12	216.50	3752.75	132.59	3237.13	114.38

other words, the yield strength of the strained material is increased to σ^*_{yp}. This effect can be evaluated by Equation 15.

$$\text{Strain hardening effect} = \int_c^{c+\rho_{cr}} (\sigma^*_{yp}(x) - \sigma_y)\,dx \tag{15}$$

The other reason is compressive residual stresses. Dahl [11] had studied the influence of plastic zone size on the fracture toughness value. He concluded that fracture toughness increased with plastic zone size. Within the plastic zone size the compressive residual stresses are the main reason to increase the critical stress intensity factor.

The residual stresses between the crack tip and $c + \rho_{cr}$ can affect the load P in Equation 14. Compressive residual stress must be compensated by external load which makes the fracture load P increase. Conversely, tensile residual stress has an inverse effect on fracture load. This effect is equal to:

$$\text{Residual stresses effect} = \int_c^{c+\rho} R(x)\,dx \tag{16}$$

where $R(x)$ is elastic/plastic stress distribution after unloading.

For theoretical calculation, the critical plastic zone must be determined first. Burdekin [16] used the Dugdale approach and has derived Equation 17

$$\begin{aligned}\delta &= \frac{8\sigma_y a}{\pi E}\log\sec\frac{\pi\sigma}{2\sigma_y}\\ &= \frac{8\sigma_y a}{\pi E}\left(\frac{1}{2}\left(\frac{\pi}{2}\frac{\sigma}{\sigma_y}\right)^2 + \frac{1}{12}\left(\frac{\pi}{2}\frac{\sigma}{\sigma_y}\right)^4 + \ldots\right)\end{aligned} \tag{17}$$

for a nominal stress value less than $0.75\sigma_y$, a reasonable approximation for δ (crack opening displacement), using only the first term of this series is

$$\delta = \frac{\pi\sigma^2 a}{E\sigma_y} \tag{18}$$

For a through-thickness crack of length $2a$,

$$K_I = \sigma(\pi a)^{1/2} \tag{19}$$

thus

$$\delta E\sigma_y = K_I^2 \tag{20}$$

Since $E = \sigma_y/\epsilon_y$, the following relation exists:

$$\frac{\delta}{\epsilon_y} = \left(\frac{K_I}{\sigma_y}\right)^2 \tag{21}$$

By substituting Equation 18 into Equation 19 to eliminate σ, at the onset of crack instability, we can get Equation 22

$$\frac{\delta_{cr}}{\epsilon_y} = \left(\frac{K_c}{\sigma_y}\right)^2. \tag{22}$$

From the Dugdale approach

$$\begin{aligned}\frac{a}{a+\rho} &= \cos\frac{\pi\sigma}{2\sigma_y}\\ &= 1 - \frac{1}{2!}\left(\frac{\pi\sigma}{2\sigma_y}\right)^2 + \frac{1}{4!}\left(\frac{\pi\sigma}{2\sigma_y}\right)^4 - \ldots.\end{aligned} \tag{23}$$

Neglecting higher order term, ρ is found as:

$$\rho = \frac{\pi^2\sigma^2 a}{8\sigma_y^2} = \frac{\pi K_I^2}{8\sigma_y^2} \tag{24}$$

By substituting Equation 20 into Equation 24, and at the onset

$$\rho_{cr} = \frac{\pi E}{8\sigma_y}\delta_{cr} \tag{25}$$

Equation 25 is identical with the limit form of ρ for $\sigma/\sigma_y \to 0$ on the basis of a Dugdale model, and its general applicability, irrespective of σ/σ_y value, have been verified experimentally [15]. For the material used in our studies, experimental result of K_c for $M = 0.244$ is equal to 116 kg mm$^{-3/2}$. True value of K_c is calculated by iteration and to be 114 kg mm$^{-3/2}$.

$$\rho_{cr} = \frac{\pi\cdot 114^2}{8\cdot 39.87} = 3.21\text{ mm}$$

Let

$$A = 2t\int_c^{c+\rho_{cr}} (\sigma^*_{yp}(x) - \sigma_y)\,dx$$

$$B = -2t\int_c^{c+\rho_{cr}} R(x)\,dx$$

$P_a = P_{ex} - A - B$ where P_{ex} is the experimental fracture load. P_a is the true fracture load which is subtracted $A + B$ from P_{ex}. From Equation 14,

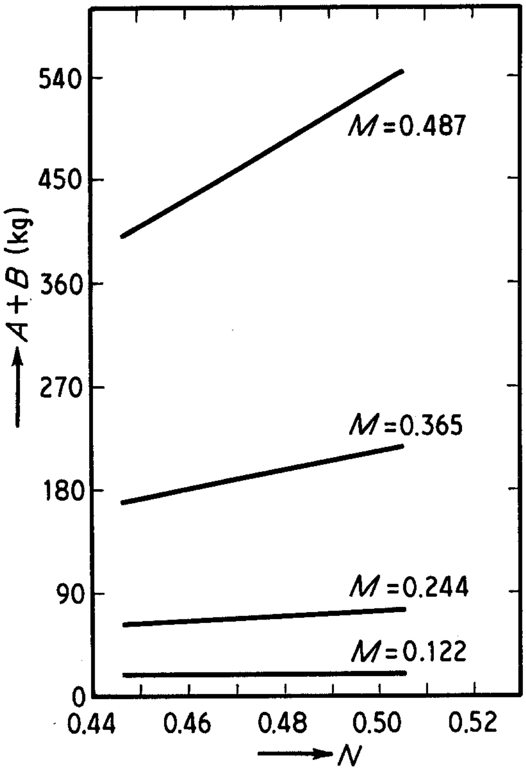

Figure 7 The effects of strain hardening and compressive residual stress $A + B$ against crack length coefficient N.

true critical stress intensity factor K_{ca} is

$$K_{ca} = \frac{P_a}{P_{ex}} K_c \qquad (26)$$

$A + B$ expresses the double effects of strain hardening and compressive residual stresses. Fig. 7 shows the curves of $A + B$ against relative crack length N for various values of gross stress coefficient M. The influences of a large crack length on $A + B$ with a small value of M are almost the same as a small crack length. But the influences of crack length are more significant as M increases. Theoretical calculations are compared with experimental results in Table II. The three P_a values of different applied gross stresses are very close. The average of actual fracture load is $P_{av} = 3211.08$ Kg. The percentage error of $(P_a - P_{av})/P_{av} \times 100\%$ for the three stress coefficients 0.244, 0.365 and 0.487, are 0.023%, -0.789% and 0.81125%, respectively. These values are significantly lower than experimental values $(P_{ex} - P_{av})/P_{av} \times 100\% =$ 2.243%, 5.651%, 16.869%. It is shown that the present model is suitable to calculate the effect of precrack load on the critical stress intensity factor measurement. True K_c values can be obtained under arbitrary fatigue loading conditions.

5. Conclusions

A study is made on the influence of different precracking load on the critical stress intensity factor under plane stress condition. The results obtained are summarized as follows:

1. Analytical results are closely matched with the experimental data.
2. Plastic zone size $(D_2' - c)$ calculated in this paper coincide with Rice's result for small crack length.
3. The effect of precracking load on the K_c value can be explained through the strain hardening effect and compressive residual stress within the plastic zone size.
4. The true K_c-value can be obtained by subtracting the combined load differences due to strain hardening and compressive residual stress from the experimental result under arbitrary fatigue loading conditions.

References

1. G. R. IRWIN, *J. Appl. Mech.* **82** (1960) 417.
2. M. L. WILLIAM, *ibid.* **79** (1972) 108.
3. W. ELBER, *Eng. Fract. Mech.* **2** (1970) 37.
4. N. J. I. ADAMS, *ibid.* **4** (1957) 543.
5. D. POST, *Proc. Soc. Exp. Stress Anal.* **12** (1954) 99.
6. J. TIROSH and A. LADELSKI, *Eng. Fract. Mech.* **12** (1980) 453.
7. J. R. RICE, *ASTM STP* **415** (1967) 247.
8. C. L. HO, O. BUCK and H. L. MARCUS, *ibid.* **536** (1973) 5.
9. W. ELBER, *Eng. Fract. Mech.* **2** (1970) 37.
10. K. M. LAL, *Trans. ASME, JEMT* **97** (1975) 284.
11. W. DAHL and W. B. KRETZSCHMANN, *Fracture* **2** (1977) 19.
12. H. M. WESTERGAARD, *J. Appl. Mech.* **61** (1939) A49.
13. E. S. JOHN and F. B. WILLIAM, *ASTM STP* **381** (1965) 133.
14. F. B. WILLIAM and E. S. JOHN, *ibid.* **410** (1966) 1.
15. F. KOSHIGA, University of Tokyo Press, Tokyo (1973) 283.
16. F. M. BURDEKIN and D. E. W. STONE, *J. Strain Anal.* **1** (1966) 145.

Received 25 August
and accepted 13 September 1982